Level structure of ^{57}Mn from a ^{55}Mn$(t,p)^{57}$Mn reaction study and a mixed-configuration shell model calculation

J. F. Mateja* and C. P. Browne
University of Notre Dame,† Notre Dame, Indiana 46556

C. E. Moss
Los Alamos Scientific Laboratory,‡ Los Alamos, New Mexico 87545

J. B. McGrory
Oak Ridge National Laboratory,§ Oak Ridge, Tennessee 37830

(Received 3 December 1976)

Twenty-seven levels below 2.7 MeV excitation in ^{57}Mn have been identified using the ^{55}Mn$(t,p)^{57}$Mn reaction. Of these levels 18 were not reported in an earlier ^{54}Cr$(\alpha,p)^{57}$Mn and ^{54}Cr$(\alpha,p\gamma)^{57}$Mn work. From a distorted-wave Born approximation analysis of the angular distributions for states up to 2.1 MeV, the $J = 5/2$ ground state spin was confirmed and $J = 5/2$ and (11/2) spin assignments were made to levels at 1837 and 1916 keV, respectively. Further, the L values extracted from the ^{55}Mn$(t,p)^{57}$Mn angular distributions were consistent with all of the tentative spin assignments given in the ^{54}Cr$(\alpha,p\gamma)^{57}$Mn study. The ground state Q value is 7438.2 ± 3.6 keV. A shell model calculation for ^{57}Mn was also attempted. A ^{48}Ca core was assumed with the valence protons restricted to the $f_{7/2}$ subshell and the valence neutrons allowed to occupy the $2p_{3/2}$, $1f_{5/2}$, and $2p_{1/2}$ subshells. The agreement between the experimental and predicted level schemes is extremely good to 2 MeV. Above 2 MeV where core and valence particle excitations are expected, the model begins to break down since these configurations were not included in the model's configuration space. The shell model wave functions were also used to calculate spectroscopic amplitudes for two nucleon transfer reactions. The quantitative agreement between the predicted strengths and the strengths extracted from the experiment for the ^{55}Mn$(t,p)^{57}$Mn reaction is satisfactory.

[NUCLEAR REACTIONS ^{55}Mn(t,p), $E(t)=17.0$ MeV, Q3D spectrograph; measured excitation energies, $\sigma(\theta,E_p)$, DWBA analysis; ^{57}Mn deduced L, J, π, enhancement factors; shell model calculation.]

INTRODUCTION

Until the recent ^{54}Cr$(\alpha,p\gamma)^{57}$Mn study[1] little was known either experimentally or theoretically about the ^{57}Mn level structure. That work raised several questions about this nucleus which motivated the present study. In terms of a spherical shell model ^{57}Mn may be described as having three holes in the proton $1f_{7/2}$ subshell. Other nuclei with either three holes or three particles in the $f_{7/2}$ subshell are divided into two distinct groups with marked differences in both level sequence and in electromagnetic transition rates depending upon whether or not the complementary shell is closed.[2,3] Since ^{57}Mn has four neutrons outside the $f_{7/2}$ subshell, the question arises as to the completeness of the closure of the $2p_{3/2}$ subshell. Depending upon the significance of the $2p_{3/2}$ subshell closure, the structure of ^{57}Mn could resemble either set of the $(f_{7/2})^3$ nuclei or neither. In our previous work eight excited states below 2.24 MeV were identified using the ^{54}Cr(α,p) reaction and tentative spin assignments were made for the lowest five states with the ^{54}Cr$(\alpha,p\gamma)$ reaction. From these results the structure of ^{57}Mn appears to most resemble, at least with respect to level sequence and γ-ray branching, those nuclei with neither shell closed (e.g., ^{55}Mn and ^{51}Mn).[2,3] There was an indication of several weak groups between 1.4- and 2.1-MeV excitation energy in the one (α,p) spectrum taken at 24-MeV bombarding energy and $\theta = 15°$. In spectra taken at several angles with lower bombarding energy these groups could not be positively identified as leading to ^{57}Mn states because this region was obscured by groups from other Cr isotopes. If there are states in this range, it would appear that there are more levels in this region of ^{57}Mn than in the other $(f_{7/2})^{-3}$ nuclei.

From the viewpoint of a weak coupling model, one might expect more levels in this ^{57}Mn region than in the other nuclei. Consideration of the neighboring even Z isotones of ^{53}Mn and ^{55}Mn suggests that one can qualitatively account for the low-lying levels of the odd-A Mn isotopes by coupling an $f_{7/2}$ particle or hole to the low-lying states of the neighboring even Cr or Fe isotopes, respectively. This is illustrated in Fig. 1 which is

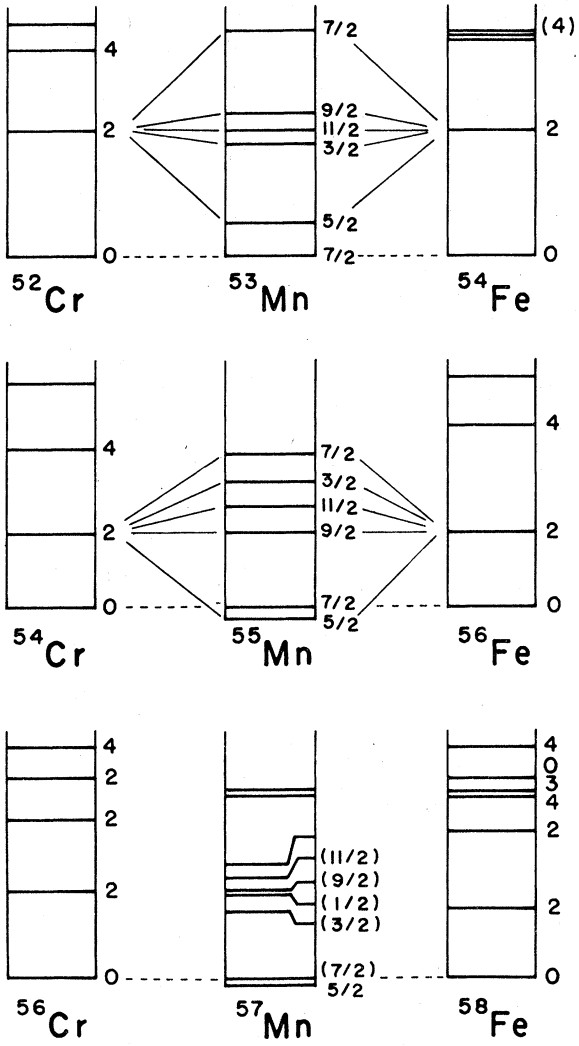

FIG. 1. Low-lying levels of ^{53}Mn, ^{55}Mn, and ^{57}Mn and of their even isotones adapted from Fig. 5 of Ref. 1. The $\frac{7}{2}\otimes 2^+$ states are easily recognizable in ^{53}Mn and ^{55}Mn since the first 2^+ state in the isotones is well isolated. One would expect, however, an additional sequence of levels with spins $\frac{3}{2}-\frac{11}{2}$ in ^{57}Mn which are not present in the other Mn isotopes because of the presence of a second 2^+ state at approximately 1.7 MeV in ^{56}Cr and ^{58}Fe.

adapted from Fig. 5 of Ref. 1. In the low-lying ^{58}Fe or ^{56}Cr spectra, however, there is a second 2^+ state which is not present in either the ^{54}Fe and ^{52}Cr or the ^{56}Fe and ^{54}Cr level schemes. A $\frac{7}{2}\otimes 2_2^+$ coupling would suggest an additional sequence of states with spin $\frac{3}{2}-\frac{11}{2}$ in the low-lying ^{57}Mn spectrum which would not be observed in the other Mn nuclei.

Since the ^{54}Cr target for the (α,p) reaction has zero spin, one assumes that the four valence protons are paired. One possible explanation for missing levels is that at higher energy the (α,p) reaction goes mainly as a direct process which excites only those ^{57}Mn states having a single proton character. If the wave functions of those levels were composed predominantly of configurations where the four valence protons of ^{54}Cr are recoupled then those levels would not be directly excited in the (α,p) reaction.

To investigate these possible recoupled $(\pi f_{7/2})^{-3}$ proton configurations in the ^{57}Mn states, we performed a ^{55}Mn(t,p) experiment. This proton configuration in ^{57}Mn should now be excited since the ^{55}Mn ground state $(J^\pi=\frac{5}{2}^-)$ already has a recoupled $(\pi f_{7/2})^{-3}$ configuration. Angular distributions for all levels up to 2.1 MeV were measured and L values extracted by comparison to distorted-wave Born approximation calculations. The L values determined in this experiment provided further evidence that the tentative spin assignments from the ^{54}Cr$(\alpha,p\gamma)$ reaction were correct.

Prior to this investigation no theoretical calculations had been performed for ^{57}Mn. Because of the success of a shell model calculation[4] for ^{55}Mn, a shell model calculation of ^{57}Mn was attempted. An inert ^{48}Ca core was assumed with the valence protons restricted to the $1f_{7/2}$ shell and the active neutrons allowed to occupy the $2p_{3/2}$, $1f_{5/2}$, and $2p_{1/2}$ shells. The results of the energy level calculations are presented and compared with the experimentally determined level structure. The shell model wave functions were used to calculate spectroscopic amplitudes for the two-nucleon transfer reaction and the theoretical cross sections are compared with the measured absolute experimental cross sections.

EXPERIMENTAL METHOD

A 17-MeV triton beam from the Los Alamos tandem Van de Graaff accelerator impinged on an 80-μg/cm^2 ^{55}Mn target with a 20-μg/cm^2 carbon backing. Beam currents were held to 50 nA at forward angles in order to reduce dead time corrections but were increased to 300 nA at back angles. Charges of 600 μC were collected at angles up to 45°, whereas 900 μC were collected from 50° to 70°. The reaction protons were momentum analyzed with the Los Alamos quadrupole-dipole-dipole-dipole (Q3D) type II spectrograph and detected at the focal surface with a helical-cathode position sensitive proportional counter.[5] The spectrograph was calibrated using the ^{59}Co$(t,p)^{61}$Co reaction because this reaction has a comparable Q value which is accurately known and the level structure of ^{61}Co is also accurately known.[6] From the ^{59}Co$(t,p)^{61}$Co data a calibration curve was obtained by using a least squares procedure to generate a fourth or-

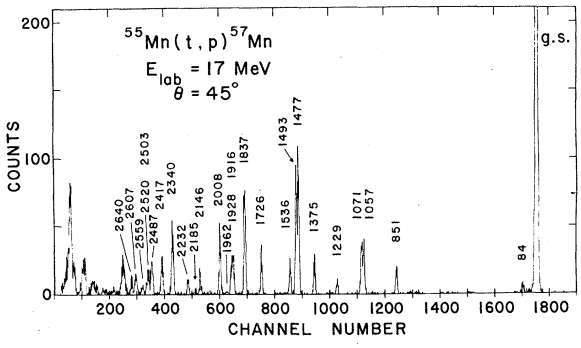

FIG. 2. Proton spectrum from the ^{55}Mn$(t,p)^{57}$Mn reaction recorded with the Los Alamos Q3D spectrograph. Excitation energies are given in keV.

der polynomial of proton momentum vs channel number. The peak centroid channels of the proton groups then were used to find the proton energies and from these the Q values and excitation energies of the ^{57}Mn states were determined. Excitation energies in ^{57}Mn were measured up to 2.7 MeV. Angular distributions, taken in 5° steps from 10° to 70°, were measured for levels up to 2.1 MeV. The 45° spectrum from this angular distribution is shown in Fig. 2. The resolution was approximately 15 keV (full width at half maximum). The ground state Q value was found to be 7438.2 ±3.6 keV. The first column in Table I shows the excitation energies measured in ^{57}Mn. The 3-KeV error quoted for the excitation energies takes into account uncertainties in beam energy and spectrograph angle, uncertainties in calibration, and random error.

Elastically scattered tritons were recorded with a silicon surface barrier detector positioned at 30° in the scattering chamber in order to detect possible changes in target thickness due to evaporation from beam heating. These elastically scattered tritons were also used to establish an absolute cross-section scale by normalizing to optical model calculations. The accuracy of the absolute cross section is estimated to be 20%.

SHELL MODEL CALCULATIONS

Only a brief summary of the underlying assumptions is given in this paper. More detailed descriptions of the model can be obtained in works by McGrory[4] and French *et al.*[7]

A ^{48}Ca closed shell core was assumed. The five valence protons were restricted to the $f_{7/2}$ shell while the four valence neutrons were allowed to move among the $2p_{3/2}$, $2p_{1/2}$, and $1f_{5/2}$ subshells. The wave functions for the ^{57}Mn states can be written as

$$\psi^J = [(\pi f_{7/2})^{(Z-20)}_{J_\pi}(\nu_{j_1} \times \nu_{j_2} \times \nu_{j_3} \times \nu_{j_4})_{J_\nu}], \quad (1)$$

where j_1 to j_4 are the orbits occupied by the four valence neutrons. Excitation energies were then calculated from a Hamiltonian of the form

$$H = (Z-20)(\pi f_{7/2}) + \epsilon(\nu_{j_1}) + \epsilon(\nu_{j_2}) + \epsilon(\nu_{j_3}) + \epsilon(\nu_{j_4}) + H_{\pi-\pi} + H_{\nu-\nu} + H_{\pi-\nu}. \quad (2)$$

TABLE I. Comparison of excitation energies and L values determined from the ^{55}Mn(t,p) experiment with ^{54}Cr$(\alpha,p)^{57}$Mn data and shell model calculations.

Present work[a]		^{54}Cr$(\alpha,p)^{57}$Mn		Shell model	
E_x (keV)	L	E_x (keV)	J	E_x (keV)	J
0	0,2,4	0	$\frac{5}{2}$	0	$\frac{5}{2}$
84	2,4	84.1 1.0	$(\frac{7}{2})$	110	$\frac{7}{2}$
851	2,4	851.1 1.0	$(\frac{3}{2})$	850	$\frac{3}{2}$
1057	2	1059.2 2.0	$(\frac{1}{2})$	1200	$\frac{1}{2}$
1071	2,4	1073.8 2.0	$(\frac{9}{2})$	1230	$\frac{9}{2}$
1229	4	1227.1 1.0	$(\frac{11}{2})$	1310	$\frac{11}{2}$
1375	2,4	1376.5 1.3		1420	$\frac{9}{2}$
1477	2,4				
1493	2,4[b]			1500	$\frac{5}{2}$
1536	2,4			1540	$\frac{7}{2}$
1726	2,4			1720	$\frac{3}{2}$
1837	0,2,4			1820	$\frac{5}{2}$
1916	4			1970	$\frac{11}{2}$
1928	2,4			1920	$\frac{3}{2}$
1962	2,4			1930	$\frac{7}{2}$
2008	2,4			2170	$\frac{9}{2}$
2146					
2185		2188.2 1.1			
2232		2234.2 1.7			
2340					
2417					
2487					
2503					
2520					
2559					
2607					
2640					

[a] The errors in the ^{55}Mn$(t,p)^{57}$Mn energies are ±3 keV.
[b] The bracket around the L values for the 1477-, 1493-, and 1536-keV levels indicates that an $L=0$ component could not be associated with any one state in particular. Therefore, the predicted $\frac{5}{2}$ spin state could not be positively identified.

The single-particle energies $\epsilon(\pi f_{7/2})$ and $\epsilon(\nu p_{3/2})$ were set to zero since only excitation energies were being calculated. Values of 2.07 and 3.96 MeV determined from the ^{49}Ca experimental spectrum[8] were used for the neutron single-particle excitations $\epsilon(\nu p_{1/2})$ and $\epsilon(\nu f_{5/2})$, respectively. Of the remaining interactions in the Hamiltonian, $H_{\pi-\pi}$ was obtained from ^{54}Fe spectroscopic data,[9] $H_{\nu-\nu}$ was taken from a shell model calculation of the Ni isotopes by Cohen *et al.*,[10] and $H_{\pi-\nu}$ was obtained from Vervier's[11] study of $N=29$ nuclei.

The two-particle transfer spectroscopic amplitudes were calculated for the ^{55}Mn$(t,p)^{57}$Mn reaction as

$$\frac{1}{(2j_f+1)^{1/2}}\left\langle j_f\,{}^{57}\mathrm{Mn}\left|\left|\frac{(a^\dagger_{j_1}\times a^\dagger_{j_2})}{(1+\delta_{j_1 j_2})^{1/2}}\right|\right|j_i\,{}^{55}\mathrm{Mn}\right\rangle, \qquad (3)$$

where j_1 and j_2 refer to the neutron shell model spin quantum numbers. The ground state ^{55}Mn wave function used in this calculation was previously determined by McGrory[4] using the Hamiltonian similar to the one outlined above. In that work it was demonstrated that the ^{55}Mn ground state wave function was well described by this model; therefore, the present calculation should provide a fairly good test of the ^{57}Mn wave functions.

DWBA ANALYSIS

A distorted-wave Born approximation (DWBA) analysis has been performed for levels below 2.1 MeV using the two nucleon transfer option of the computer code DWUCK 4.[12] Because of the lack of available triton elastic scattering data on ^{55}Mn, optical model parameters obtained from the elastic scattering of polarized tritons on ^{52}Cr were employed. This particular parameter set, measured by Hardekopf, Veeser, and Keaton,[13] was used because it not only described the elastic scattering data but also the analyzing power results. For the exit channel the global proton parameter set of Perey[14] was used. However, to obtain good phase agreement between the experimental and calculated results, the real and imaginary proton well depths had to be increased. Both the triton and proton parameters used in this analysis are listed in Table II.

The experimental cross section for the reaction $A(t,p)B$ can then be related to the cross section calculated with the code DWUCK as

$$\frac{d\sigma}{d\Omega_{\mathrm{exp}}}=\epsilon\sum\frac{2j_B+1}{2j_A+1}\frac{(T_A 1 N_A 1\,|\,T_B N_B)^2}{2J+1}$$

$$\times\sum_L N_L\frac{d\sigma}{d\Omega^{LSJ}_{\mathrm{DWUCK}}}, \qquad (4)$$

where j_A, T_A, N_A and j_B, T_B, N_B are the spin, isospin, and isospin projection for the ground state of the target and the states populated in the residual nucleus, respectively. The Clebsch-Gordan coefficient in Eq. (4) accounts for the change in isospin due to the pick up of the neutron pair. An isospin of $\frac{5}{2}$ was used for ^{55}Mn levels and $\frac{7}{2}$ for states in ^{57}Mn. The total transferred angular momentum J is equal to the transferred orbital angular momentum L for the (t,p) reaction. $d\sigma/d\Omega^{LSJ}_{\mathrm{DWUCK}}$ is the calculated differential cross section in which a coherent sum has been taken over all possible two-nucleon configurations for each L transfer.

TABLE II. Optical model parameters used in the distorted-wave analysis.

	V (MeV)	W_v (MeV)	W_s (MeV)	r_0 (fm)	a (fm)	r'_0 (fm)	a' (fm)	r_c (fm)
t	165.3	16.7		1.20	0.65	1.60	0.80	1.3
p	52.0		15.0	1.25	0.65	1.25	0.47	1.25

The spectroscopic amplitude for each configuration was calculated using the two nucleon overlap described in Eq. (3). These spectroscopic amplitudes are listed in Table III. The first two columns in this table identify the shell model state by means of predicted excitation energy and spin. Column three lists the allowed L transitions to each state. The last six columns list the results of the shell model calculation for the two-nucleon spectroscopic amplitudes.

The DWBA calculations were normalized with the procedure described by Flynn and Hanson.[15] A value for the normalization for all L transfers of 218 $\pm$33 was found[16] when accepted triton and proton optical model parameters were used in the DWBA code DWUCK. However, the use of a different set of triton and proton optical model parameters results in calculated cross sections smaller than those calculated using the Flynn and Hanson set. The magnitudes were reduced by factors of 5, 40, and 30% for the $L=0$, 2, and 4 components of the ground state transition, respectively. The value of the normalizations, N_L, was accordingly increased in size by the above amounts for all levels in ^{57}Mn to compensate for this effect.

The remaining quantity in Eq. (4), the enhancement factor ϵ, is then a measure of how well the experimental data are described by the calculation. An ϵ equal to 1 would indicate a perfect prediction.

RESULTS AND DISCUSSIONS

Comparison of the relative intensities of the ground and first excited state groups in the (α,p) and the (t,p) spectra suggests a significant difference in the type of states populated with these

TABLE III. Spectroscopic amplitudes calculated using shell model wave functions. The first two columns give the excitation energy and spin, respectively, predicted from the shell model.

E_x (keV)	J	L	Two-nucleon transfer amplitudes $(p_{3/2})^2$	$(f_{5/2})^2$	$(p_{1/2})^2$	$(p_{3/2},f_{5/2})$	$(p_{3/2},p_{1/2})$	$(f_{5/2},p_{1/2})$
0	$\frac{5}{2}^-$	0	−0.5682	−0.5813	−0.3138			
		2	−0.0893	0.1908		−0.0190	−0.1178	−0.1689
		4		−0.0445		−0.0490		
110	$\frac{7}{2}^-$	2	−0.0535	0.2077		−0.0567	−0.0280	−0.1669
		4		−0.0718		−0.1075		
850	$\frac{3}{2}^-$	2	−0.2714	−0.2017		−0.0469	−0.4288	−0.0236
		4		0.0300		−0.0826		
1200	$\frac{1}{2}^-$	2	−0.4807	−0.3320		−0.0062	−0.5841	0.0289
1230	$\frac{9}{2}^-$	2	0.1363	0.2047		−0.1073	0.1354	−0.2705
		4		−0.1165		−0.2925		
1310	$\frac{11}{2}^-$	4		−0.1286		−0.1140		
1420	$\frac{9}{2}^-$	2	0.3136	0.1630		0.1423	0.3881	0.0320
		4		−0.0859		0.2036		
1500	$\frac{5}{2}^-$	0	0.0955	−0.0820	0.0884			
		2	0.2234	0.2233		0.1045	0.2471	−0.1137
		4		−0.1690		0.2382		
1540	$\frac{7}{2}^-$	2	−0.1976	−0.1720		0.1187	−0.0140	0.3509
		4		−0.0409		0.4512		
1720	$\frac{3}{2}^-$	2	0.1209	0.1649		0.0467	0.0064	0.0044
		4		−0.1487		0.2846		
1820	$\frac{5}{2}^-$	0	−0.3765	0.2380	−0.1907			
		2	−0.3228	−0.1650		0.0536	−0.0914	0.2404
		4		−0.0581		0.3160		
1920	$\frac{3}{2}^-$	2	0.2853	0.0125		−0.2146	0.2587	−0.1643
		4		0.0455		−0.0646		
1930	$\frac{7}{2}^-$	2	−0.2339	−0.2491		0.0471	−0.0384	0.0735
		4		0.3018		−0.2152		
1970	$\frac{11}{2}^-$	4		−0.1489		0.3688		

two reactions. Figures 2 and 3 show ^{55}Mn(t,p) ^{57}Mn and ^{54}Cr$(\alpha,p)^{57}$Mn spectra from the present work and Ref. 1, respectively. In the (t,p) experiment the ground state is the most strongly populated level in the spectrum, whereas the first excited state is the most intense level in the (α,p) spectrum. This result might be explained if one looks at the wave function of the target to which the "triton" or "dineutron" is added. In the case of the ^{54}Cr(α,p) reaction, the fact that the target has $J^\pi = 0^+$ implies that both the proton and neutron subshells are coupled to zero angular momentum. Thus, since it is the spin $\frac{7}{2}$ first-excited state in ^{57}Mn which is strongly excited in the (α,p) reaction, it would appear that the (α,p) reaction simply deposits a proton into the available $f_{7/2}$ subshell of the target along with a neutron pair coupled to zero angular momentum. It is the proton single particle character of the final wave function which is primarily investigated with the (α,p) reaction.

In the case of the ^{55}Mn(t,p) reaction the situation is more difficult because of the complexity of the ^{55}Mn ground state wave function. In a simple shell model picture of ^{55}Mn the $\frac{5}{2}$ ground state spin arises from the coupling of three $f_{7/2}$ proton holes. The fact that it is the spin $\frac{5}{2}$ ground state of ^{57}Mn which is most strongly populated in the (t,p) reaction suggests that this reaction mainly excites that particular part of the final state wave function which consists of protons in the same $(f_{7/2})^{-3}$ configuration. The neutron coupling depends upon the spin of the final state.

The excitation energies of the levels observed in this experiment which are listed in column 1 of Table I, may be compared with the excitation energies measured using the (α,p) reaction[1] which are given in column 3. Eighteen levels below 2.7 MeV not reported from the (α,p) experiment,[1] were measured with the (t,p) reaction. Ten of these new levels are observed in the energy range between 1.4 and 2.15 MeV and some of these states could arise from the weak coupling of a single hole to the second 2^+ ^{58}Fe level as previously discussed. How-

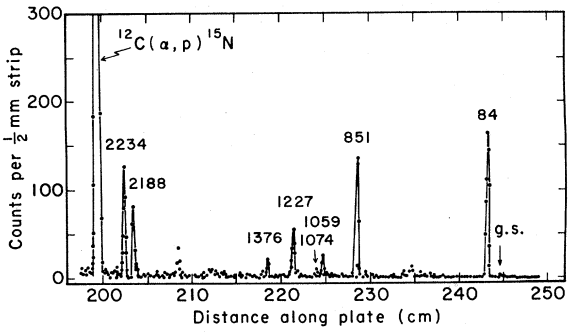

FIG. 3. Proton spectrum from the ^{54}Cr$(\alpha,p)^{57}$Mn reaction taken from Ref. 1. The angle of observation was 15.5° and the incident α energy was 24 MeV. Excitation energies are given in keV.

ever, until additional characteristics for these levels are determined, this hypothesis cannot be tested further.

Columns 1 and 5 of Table I and Fig. 4 compare the results of the shell model calculation with the experimental data. The agreement between the calculated and experimental spectrum is exceedingly good up to 2 MeV. For the first six experimental levels for which tentative spin assignments have been proposed,[1] the predicted level ordering is correct and the largest deviation between the calculated and experimental excitation energies is only 160 keV. As seen from the DWBA calculations discussed below, a definitive $\frac{5}{2}$ spin assignment to the 1837-keV level can be made because of its $L=0$ (t,p) component. Thus, it appears that this level has also been correctly predicted by the shell model. The $L=4$ character of the 1916-keV state suggests that this state has high spin. This would agree with the $\frac{11}{2}$ spin assignment for a state at 1970 keV predicted by calculation.

The calculation, predicting two levels around 1.5 MeV does not account for the three levels seen experimentally. It is possible that one of these levels arises because of proton excitations into the $2p_{3/2}$ subshell. These states would not be predicted by the calculation since the protons were restricted to the $f_{7/2}$ subshell. The appearance of such states has been previously discussed by McGrory[4] for other nuclei in this mass region.

Care must be taken when interpreting the results of shell model calculations. Because one uses an effective interaction, it is conceivable that the wrong Hamiltonian and the wrong wave functions have predicted the correct energy level spacings and spin sequence. A more sensitive test of the wave functions is the calculation of the spectroscopic amplitudes for nuclear transfer reactions. The test is particularly sensitive in the case of two-nucleon transfer reactions since both constructive and destructive interference may occur between the many possible two-nucleon configurations. This interference strongly effects the magnitude and shape of the predicted cross section.

Angular distributions using the spectroscopic amplitudes listed in Table III were generated with the

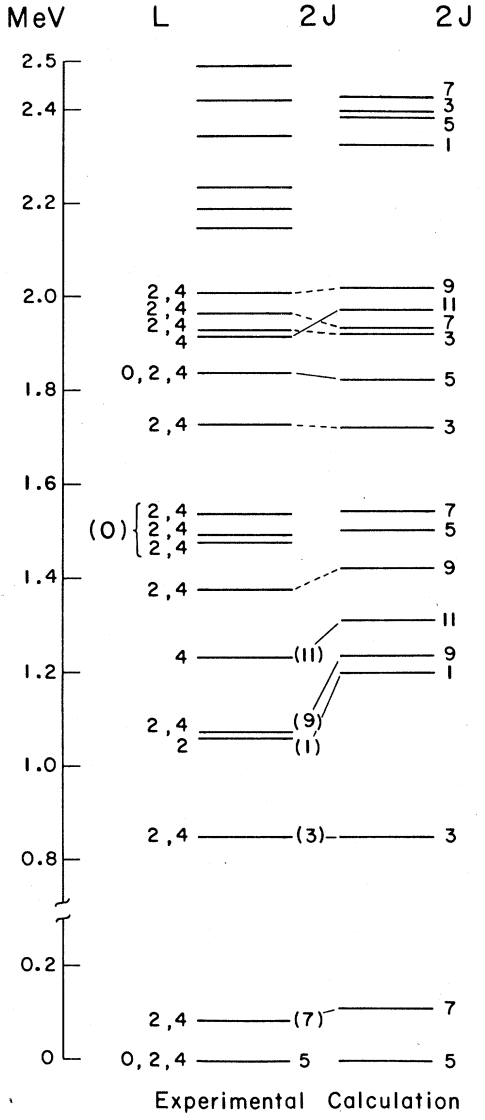

FIG. 4. Comparison of experimental and shell model predicted level spectra. The solid lines connecting shell model and experimental states indicate shell model states for which definite correspondence with experimental levels can be made based upon tentative experimental spin assignments. Dashed lines indicate correspondence between shell model and experimental levels based only upon agreement in excitation energies. Not all states found in this work are shown. Five more states above 2.5 MeV are listed in Table I.

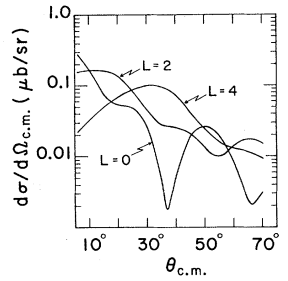

FIG. 5. Comparison of pure $L=0$, 2, and 4 angular distributions.

microscopic two-nucleon transfer option of the computer code DWUCK4. These cross sections were normalized using the method of Flynn and Hanson[15] discussed previously. It should be noted that the shapes of the calculated distributions were configuration and Q value independent but depended strongly on the L transfer. For reference, the pure L shapes are shown in Fig. 5. Since the spectroscopic amplitudes of Table III were used, the contribution from different L components for a particular state is that determined by the shell model calculation. For the ^{57}Mn states Figs. 6–8 present a comparison of the experimental angular distributions with the theoretical curves calculated from Eq. (4).

Three general observations can be made when comparing the DWBA results and the experimental data. First, the shape of the angular distributions for the essentially pure or pure $L=0$ and $L=2$ transfer states is well fitted by the distorted-wave analysis. This is apparent for the ground state where the $L=0$ distribution is dominant and for the pure $L=2$ transition state at 1057 keV. The shape of the $L=4$ angular distribution, as evidenced by the 1229-keV level, is not as well fitted by the calculation. The primary maximum around 30° seems to be described well; however, the experimental points at back angles lie above the calculated curve. One should note that the cross section for this state is small and other processes such as compound or two step may be important.

Second, the angular distributions are well reproduced using the spectroscopic amplitudes predicted by the shell model calculation. For example, in Fig. 6 the angular distributions for the 84-, 851-, and 1071-keV states are all described in terms of a combination of $L=2$ and 4 transfer components. For the 84-keV level the $L=4$ component of the experimental angular distribution is dominant and is well reproduced, at least at forward angles, by the DWBA calculation. On the other hand, for the 851- and 1071-keV levels it is the $L=2$ component of the angular distribution which is experimentally strong and also correctly reproduced in the distorted-wave analysis. Similarly when one mixes three L transfer components for the 1837-keV state (Fig. 7), the experimental angular distribution is reasonably well reproduced by the shape of the calculated curve. The fact that this curve contains an $L=0$ component and does fit the forward angle data where the $L=0$ component is strongest, is evidence that this is a spin $\frac{5}{2}$ state. Unfortunately, the predicted $\frac{5}{2}$ spin state around 1.5 MeV cannot be identified in this manner. Since amplitudes for the configurations of the $L=0$ component of this

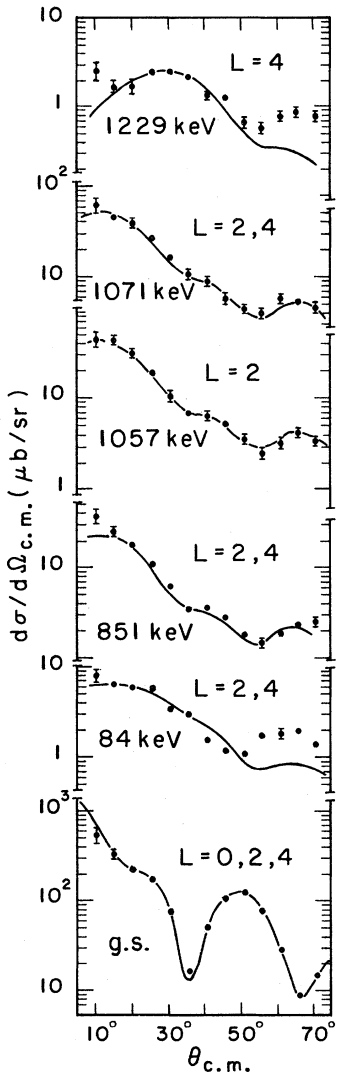

FIG. 6. Angular distributions for the ^{55}Mn$(t,p)^{57}$Mn reaction. The curves are results of DWBA calculations using spectroscopic amplitudes from Table III. The L admixtures are those predicted by the shell model, but the over-all magnitude has been adjusted independently to facilitate shape comparison. The value of this adjustment determines ϵ of Eq. (4).

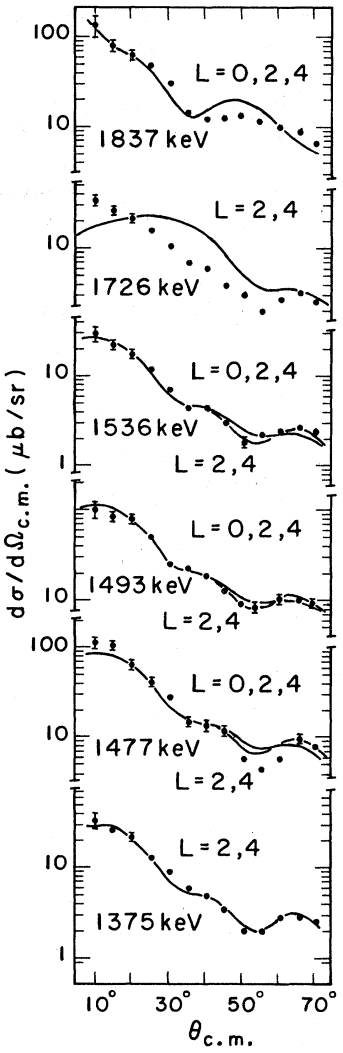

FIG. 7. Angular distributions for the ^{55}Mn$(t,p)^{57}$Mn reaction. The curves are results of DWBA calculations using spectroscopic amplitudes from Table III. The L admixtures are those predicted by the shell model, but the over-all magnitude has been adjusted independently to facilitate shape comparison. The value of this adjustment determines ϵ of Eq. (4).

state destructively interfere while those of the $L=2$ component primarily constructively add (see Table III), there is no strong $L=0$ character for this $\frac{5}{2}$ state. As can be seen in Fig. 7 where the shapes for both the $\frac{5}{2}$ and $\frac{7}{2}$ spin state have been shown for all the states around 1.5 MeV, the $\frac{5}{2}$ spin state cannot be uniquely identified.

Only the experimental shape of the 1726-keV state is not well reproduced by the distorted-wave calculation employing the shell model spectroscopic amplitudes. One explanation is that the shell model state may not be associated with the correct experimental state since the spin for the 1726-keV state has not been determined. Another explanation involves the $\frac{3}{2}$ spin predicted for this level. Because of the proximity of the $2p_{3/2}$ subshell and the fact that excitations to this subshell would significantly affect states with $\frac{3}{2}$ spins, a major component of the wave function for this state may have been neglected. If this wave function is incomplete, then it could not account correctly for the relative contributions of the various L transfers. This ambiguity of whether the state has been mismatched or is strongly affected by the $2p_{3/2}$ subshell could be partially removed if the spin for this state could be measured.

Finally, there is generally good agreement between the theoretical and experimental transition strengths for states in ^{57}Mn up to about 2 MeV. The experimental transition strengths are compared

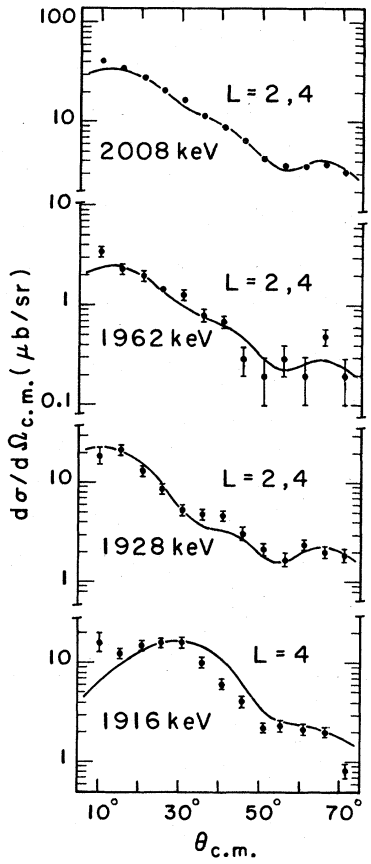

FIG. 8. Angular distributions for the ^{55}Mn$(t,p)^{57}$Mn reaction. The curves are results of DWBA calculations using spectroscopic amplitudes from Table III. The L admixtures are those predicted by the shell model, but the over-all magnitude has been adjusted independently to facilitate shape comparison. The value of this adjustment determines ϵ of Eq. (4).

TABLE IV. Magnitudes of the experimental and DWBA calculated cross sections.

Measured E_x (keV)	L	$2J$	σ_{exp} [a] (μb)	σ_{DWUCK}^{normal} [a,b] (μb)	ϵ [c]
0	0,2,4	5	1709±342	1958±294	0.87
84	2,4	7	43±9	16±2	2.74
851	2,4	3	83±17	501±75	0.16
1057	2	1	186±37	587±88	0.32
1071	2,4	9	243±49	658±99	0.37
1229	4	11	20±4	22±3	0.92
1375	2,4	9	129±26	1171±176	0.11
1477	0,2,4	5	438±88	537±81	0.82
1477	2,4	7	438±88	578±87	0.76
1493	0,2,4	5	454±91	536±80	0.85
1493	2,4	7	454±91	578±87	0.79
1536	0,2,4	5	114±21	540±81	0.21
1536	2,4	7	114±21	582±87	0.20
1726	2,4	3	143±29	55±8	2.61
1837	0,2,4	5	446±89	1135±170	0.39
1916	4	11	103±21	196±29	0.52
1928	2,4	3	88±18	516±77	0.17
1962	2,4	7	14±3	271±41	0.05
2008	2,4	9	193±39	597±90	0.32

[a] σ_{exp} and σ_{DWUCK}^{normal} were obtained by summing the cross section from 10° to 70° in 5° steps.

[b] σ_{DWUCK}^{normal} was normalized according to the method described in Refs. 15 and 16.

[c] The quantity ϵ [the enhancement factor of Eq. (4)] is a measure of how well the experimental data are described by the calculation.

with the calculated strengths in columns 4 and 5 of Table IV. The notable features of the experimental data which are well reproduced by the calculation are the strong ground state strength and the very weak transition strength to states at 84 and 1229 keV. The remaining levels are, for the most part, all moderately strongly excited and usually predicted to within a factor of 3. For the states around 1.5 MeV, there is not a sufficient difference in the magnitudes of either the experimental or calculated strength to identify the $\frac{5}{2}$ spin state in this group.

In summary, better agreement would probably be achieved if proton and neutron excitation out of the $f_{7/2}$ subshell were allowed. Nevertheless, the agreement appears good enough to suggest that the principle components of the wave functions for these states have been correctly predicted in this analysis.

SUMMARY AND CONCLUSION

In this investigation, the excitation energies of 26 levels below 2.7 MeV were measured. Of these levels, 18 had not been reported in earlier ^{54}Cr$(\alpha,p)^{57}$Mn work.[1] From the (t,p) angular distributions definitive $\frac{5}{2}^-$ spin assignments could be made to the ^{57}Mn ground state and a state at 1837 keV because of the $L=0$ components of these angular distributions. In addition, no discrepancies were found between the tentative spin assignments of Ref. 1 and the spin limitations imposed by the L values extracted from the (t,p) angular distributions. Comparison of the relative intensities of the ground and first excited state groups in the (α,p) and (t,p) spectra suggests that the (t,p) reaction primarily populates the recoupled $(\pi f_{7/2})^{-3}$ character of the ^{57}Mn states, whereas the 24-MeV (α,p) reaction data mainly probe the proton single-particle nature of these levels.

A shell model calculation in which a ^{48}Ca core was assumed has been performed. The predicted excitation energies are in strikingly good agreement with the experimental spectrum up to 2 MeV. Further, where comparisons could be made with experimental spin assignments, there do not appear to be any discrepancies between the calculated and experimental results. Only one level below 2 MeV (that at 1.5 MeV) is not accounted for by the model. This suggests that restricting the protons to the $f_{7/2}$ subshell and not allowing core excitations may be too strict a limitation even at low excitation energies.

As an additional test, the wave functions generated in this calculation were used to predict the strength of the (t,p) two-nucleon transfer reaction. The calculated spectroscopic amplitudes were incorporated into a DWBA analysis to predict the shape and magnitude for angular distributions of states up to 2.1 MeV in ^{57}Mn. The calculated spectroscopic amplitudes described the experimental absolute cross sections well. In general, the strongest and weakest transitions were accurately described. In other cases, the experimental magnitude was usually predicted to within a factor of 3. The agreement between the experimental and calculated angular distributions is good enough to suggest that the principle components of these wave functions have been correctly predicted by this model.

The low-lying level structure of ^{57}Mn appears to maintain the $(f_{7/2})^{\pm 3}$ configuration of those nuclei which have neither the proton or neutron shell filled. The states formed from this $(f_{7/2})^{\pm 3}$ configuration have been connected with dashed lines in Fig. 9. As can be seen the spin $\frac{5}{2}$, $\frac{7}{2}$, $\frac{9}{2}$, and $\frac{11}{2}$ states have energies in ^{57}Mn approximately equal to their counterparts in the other nuclei. The $J=\frac{3}{2}$, 851-keV state, which would also be a member of the $(f_{7/2})^{\pm 3}$ group, drops significantly in energy with increasing mass number from ^{51}Mn to ^{57}Mn. However, it has been noted that the $J=\frac{3}{2}$ lev-

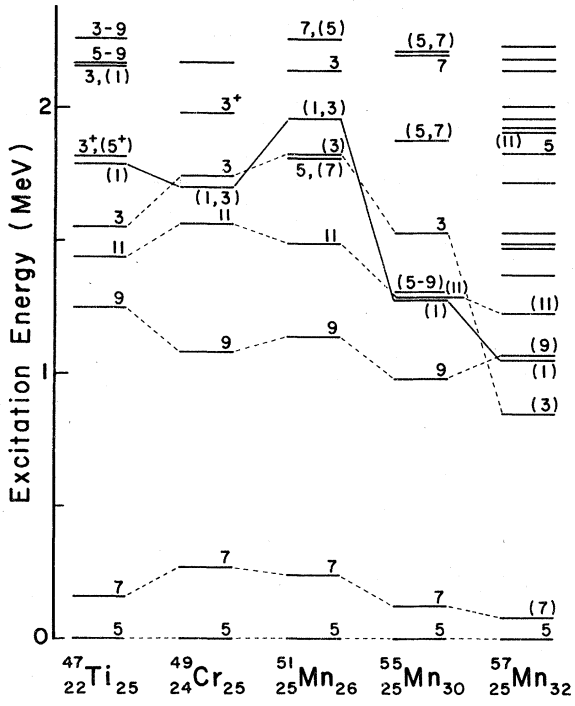

FIG. 9. Low-lying level structure of nuclei which have the $(f_{7/2})^{\pm 3}$ configuration. The states connected with a solid line have tentative assignments of $J=\frac{1}{2}$. If the states which have tentative $J=\frac{1}{2}$ assignments are indeed correct, then the $J=\frac{1}{2}$ level seems to exhibit the same change in excitation energy with increasing mass number as the $J=\frac{3}{2}$ state. The ^{55}Mn results were taken from Ref. 17, ^{51}Mn results from Refs. 18 and 19, the ^{49}Cr results from Ref. 20, and the ^{47}Ti results from Ref. 21.

el is subject to strong configuration mixing due to the proximity of the $2p_{3/2}$ subshell.[2] This may account for the strong variation in excitation energy with mass number for this state.

The only real anomaly in the low-lying ^{57}Mn structure, or as it would have appeared, is the $J=\frac{1}{2}$ state at 1059 keV. This state cannot be a member of the $(f_{7/2})^{\pm 3}$ group of low-lying states since a $J=\frac{1}{2}$ is not allowed by the vector coupling of three $\frac{7}{2}$ particles. In terms of the weak coupling model, this level would have to be built on the first 4^+ state in any of the even isotones of these nuclei. The latest mass 55 Nuclear Data Sheets compilation[17] indicates the possible existence of a 3-keV triplet at about 1290 keV in ^{55}Mn. One member of this group is a $J=\frac{1}{2}$ state. If the tentatively assigned $J=\frac{1}{2}$ states in the five nuclei of Fig. 9 do indeed have $J=\frac{1}{2}$, then this state seems to demonstrate the same type of variation in excitation energy with mass number as the $J=\frac{3}{2}$ state discussed above. This change in excitation energy would indicate that this state may be strongly affected by configuration mixing because of the $2p_{1/2}$ proton subshell.

Between 1.2 and 2 MeV, there are many more levels in ^{57}Mn than in any of the other odd-A nuclei. It appears that most of these additional levels in ^{57}Mn can be explained in terms of the weak coupling model. If the even isotones of the odd-A Mn isotopes are considered, one sees that in the even isotones of ^{57}Mn, ^{58}Fe, and ^{56}Cr, an additional 2^+ state has moved into the 1.6-MeV region in the ^{58}Fe and ^{56}Cr spectra (see Fig. 1). A $J=\frac{7}{2}$ particle coupled to this additional 2^+ state would produce a sequence of states with spins from $\frac{3}{2}$ to $\frac{11}{2}$ which would not be present in any of the other odd-A Mn nuclei.

ACKNOWLEDGMENTS

We are grateful to Dr. E. R. Flynn for numerous helpful discussions and to all of the Q3D group for their assistance. In addition one of us (JFM) would like to thank Dr. P. L. Jolivette for his assistance throughout the entire experiment.

*Present address: Department of Physics, Florida State University, Tallahasee, Florida 32306.
†Work supported by the National Science Foundation under Grant No. PHY 71-02582A5.
‡ Work supported by the U.S. Energy Research and Development Administration.
§Research sponsored by the U.S. Energy Research and Development Administration under Contract with Union Carbide Corporation.

[1]J. F. Mateja, G. F. Neal, J. D. Goss, P. R. Chagnon, and C. P. Browne, Phys. Rev. C 13, 118 (1976).
[2]B. P. Hichwa, J. C. Lawson, and P. R. Chagnon, Nucl. Phys. A215, 132 (1973).
[3]J. W. Noé, R. W. Zurmühle, and D. P. Balamuth, Bull. Am. Phys. Soc. 18, 653 (1973); Nucl. Phys. A277, 137 (1977).
[4]J. B. McGrory, Phys. Rev. 160, 915 (1967).
[5]E. R. Flynn, S. Orbeson, J. D. Sherman, J. W. Sunier, and R. Woods, Nucl. Instrum. Methods 128, 35 (1975).
[6]J. F. Mateja, J. A. Bieszk, J. T. Meek, J. D. Goss, A. A. Rollefson, P. L. Jolivette, and C. P. Browne, Phys. Rev. 13, 2269 (1976); P. L. Jolivette, J. D. Goss, G. L. Marolt, A. A. Rollefson, and C. P. Browne, *ibid.* 10, 2449 (1974).
[7]J. B. French, E. C. Halbert, J. B. McGrory, and S. S. M. Wong, in *Advances in Nuclear Phys.*, edited by M. Baranger and E. Vogt (Plenum, New York, 1970), Vol. III.
[8]E. Kashy, A. Sperduto, H. A. Enge, and W. W. Buechner, Phys. Rev. 135, B865 (1964).
[9]M. F. Thomas, A. R. Poletti, and M. A. Grace, Nucl. Phys. 78, 561 (1966).
[10]S. Cohen, R. D. Lawson, M. H. MacFarlane, S. Pendya,

and M. Soga (unpublished).
[11]J. Vervier, Nucl. Phys. 78, 497 (1966).
[12]P. D. Kunz (private communication).
[13]R. A. Hardekopf, L. R. Veeser, and P. W. Keaton, Jr., Phys. Rev. Lett. 35, 1623 (1975).
[14]F. G. Perey, Phys. Rev. 131, 745 (1963).
[15]E. R. Flynn and O. Hanson, Phys. Lett. 31B, 135 (1970).
[16]E. R. Flynn, J. D. Sherman, N. Stein, D. K. Olsen, and P. J. Riley, Phys. Rev. C 13, 568 (1976).
[17]D. C. Kocher, Nucl. Data Sheets 18, 463 (1976).
[18]I. Forsblom, Phys. Scr. 6, 309 (1972).
[19]R. W. Tarara, J. D. Goss, P. L. Jolivette, G. F. Neal, and C. P. Browne, Phys. Rev. C 13, 109 (1976).
[20]R. W. Zurmühle, D. A. Hutcheon, and J. J. Weaver, Nucl. Phys. A180, 417 (1972).
[21]J. J. Weaver, M. A. Grace, D. F. H. Start, R. W. Zurmühle, D. P. Balamuth, and J. W. Noé, Nucl. Phys. A196, 269 (1972).